**Düzce University Journal of Science & Technology**

*Research Article*

# Catalytic Pyrolysis of Grape Seed Waste: Characterization of Bio-Char and Bio-Oil

Koray ALPER [a,*]

[a]*Department of Environmental Protection Technologies, Zonguldak Bulent Ecevit University, 67100, Zonguldak, TÜRKİYE*

** Corresponding author's e-mail address: korayalper@beun.edu.tr*

DOI: 10.29130/dubited.1597245

## ABSTRACT

The utilization of biomass waste for biofuel production through pyrolysis has emerged as a promising approach to combat global warming. This process enables the generation of bio-char, bio-oil, and bio-gas using a straightforward and cost-efficient method. Among the biomass residues in Turkey, grape seeds from the food processing industry offer considerable potential as an alternative energy source. This research explores the characteristics of bio-oil and bio-char produced from grape seed pyrolysis conducted in a nitrogen atmosphere (inert gas) at temperatures ranging from 500 to 800 °C. Additionally, the effects of Purmol CTX and Clinoptilolite catalysts on product yield and composition were examined in optimal experimental results. Results indicate that higher pyrolysis temperatures yield carbon-dense bio-chars with elevated heating values and minimal impurities, rendering them viable as solid biofuels. Meanwhile, the bio-oils consist of compounds such as phenols, alkanes, alkenes, alkyls, and acids, positioning them as eco-friendly candidates for sustainable biofuel applications.

***Keywords:*** *Pyrolysis, Grape seed, Bio-char, Bio-oil*

# Üzüm Çekirdeği Atıklarının Katalitik Pirolizi: Biyo-Kömür ve Biyo-Yağın Karakterizasyonu

## Öz

Biyokütle atıklarının piroliz yoluyla biyoyakıt üretiminde kullanılması, küresel ısınmayla mücadelede umut verici bir yaklaşım olarak ortaya çıkmıştır. Bu süreç, biyo-kömür, biyo-yağ ve biyo-gaz gibi ürünlerin basit ve maliyet açısından etkin bir yöntemle üretilmesini sağlar. Türkiye'deki biyokütle atıkları arasında, gıda işleme endüstrisinden elde edilen üzüm çekirdekleri, alternatif bir enerji kaynağı olarak önemli bir potansiyele sahiptir. Bu araştırma, 500 ile 800 °C arasındaki sıcaklıklarda azot atmosferinde (inert gaz) gerçekleştirilen üzüm çekirdeği pirolizinden elde edilen biyo-yağ ve biyo-kömürlerin özelliklerini incelemektedir. Ayrıca, optimum deney sonuçlarında *Purmol CTX ve Klinoptilolit* katalizörlerinin ürün verimin ve içeriğine etkisi incelenmiştir. Sonuçlar, daha yüksek piroliz sıcaklıklarının, karbon bakımından yoğun, yüksek ısıl değerli ve minimum safsızlık içeren biyo-kömürler ürettiğini ve bunların katı biyo-yakıt olarak kullanıma uygun olduğunu göstermektedir. Aynı zamanda, bio-yağların fenoller, alkanlar, alkenler, alkil grupları ve asitler gibi bileşikler içerdiği ve bu nedenle sürdürülebilir biyo-yakıt uygulamaları için çevre dostu adaylar olarak değerlendirilebileceği belirtilmektedir.

***Anahtar Kelimeler:*** *Piroliz, Üzüm çekirdeği, Biyo-kömür, Biyo-yağ.*

Received: 07/12/2024, Revised: 15/12/2024, Accepted: 03/01/2025

# I. INTRODUCTION

The growing demand for sustainable energy solutions and the escalating environmental challenges have propelled the adoption of renewable energy sources, such as wind, solar, hydropower, and biomass, in both scientific research and industrial applications [1]. Among these options, biomass stands out as a versatile energy source due to its capability to be directly converted into biofuels and its role in reducing waste [2]. Biomass pyrolysis, a thermal decomposition process conducted at high temperatures in an oxygen-free environment, generates valuable products, including bio-char, bio-oil, and bio-gas. Liquid products from pyrolysis, accounting for 30-70% of the total yield, predominantly consist of oxygenated compounds and are typically divided into two fractions based on their water solubility: a dense, viscous tar fraction (water-insoluble) and bio-oil (water-soluble) [3, 4].

The structural composition of biomass, which includes cellulose, hemicellulose, lignin, and small quantities of other organic matter, dictates its pyrolysis behavior. While hemicellulose and cellulose decompose rapidly at lower temperatures, lignin exhibits greater thermal stability, breaking down at higher temperature ranges [5]. Experimental factors, such as pyrolysis temperature, heating rate, and pressure, significantly influence the degradation rates and yields of these components [6].

Pyrolysis, typically conducted in an inert atmosphere of nitrogen or argon, has emerged as one of the most efficient thermo-chemical processes for biofuel production [7, 8]. This process enables the conversion of biomass into a range of high-value products, including solid bio-char, liquid bio-oil, and gaseous biofuels [9]. High heating rates up to temperatures below 650°C, combined with rapid quenching, promote the formation of liquid products while minimizing char and gas production; this process is commonly known as "flash pyrolysis." In contrast, high heating rates to temperatures above 650°C favor the production of gaseous products over liquids. Slow heating rates and low maximum temperatures, on the other hand, maximize char yield [10].

Compared to raw biomass, bio-oil offers higher energy density and ease of transport and storage [11]. It also serves as a precursor for various industrial chemicals, such as food flavorings, specialty chemicals, resins, agricultural inputs, and emission control agents [12]. Comprising a diverse array of organic compounds (such as alkanes, aromatic hydrocarbons, phenols, ketones, esters, and ethers) bio-oil demonstrates versatility, with a molar H/C ratio exceeding 1.5 [13]. However, despite its potential, converting bio-oil into transportation fuels remains economically unviable [12]. Solid bio-char, another pyrolysis by-product, finds applications in the chemical, pharmaceutical, and food industries due to its structural and reactive properties, as well as its low sulfur and phosphorus content [14].

Numerous studies underscore the impact of pyrolysis parameters on the yields and characteristics of these products. Fruit waste, in particular, represents a promising biomass resource for biofuel production. For instance, Raja et al. conducted fluidized bed flash pyrolysis experiments on Jatropha oil cake to examine the effects of particle size, pyrolysis temperature, and nitrogen gas flow rate on pyrolysis yields. The highest oil yield, 64.25 wt%, was achieved at a pyrolysis temperature of 500°C, a particle size of 1.0 mm, and a nitrogen gas flow rate of 1.75 $m^3/h$. The resulting pyrolysis oil, identified as a potential biofuel, had a calorific value of 19.66 MJ/kg, which is approximately half the energy content of diesel [15]. Similarly, Xu et al. investigated the fuel properties of pyrolysis products obtained from grape residues, specifically grape skins and a mixture of grape skins and seeds. The study utilized a pilot-scale bubbling fluidized bed pyrolyzer, conducting experiments across a temperature range of 300 °C to 600 °C and varying vapor residence times (2.5, 5, and 20 seconds). The primary objective was to analyze the pyrolysis behavior of these residues, with a focus on product yields and heat requirements. To achieve the most favorable pyrolysis conditions for a sustainable process in terms of energy efficiency, the optimum temperature is 550 °C for grape skins and 450 °C for the mixture of grape skins and seeds [11]. Pütün et al. demonstrated that pyrolyzing olive waste at 400-700 °C could produce petroleum-like products. Experimental studies revealed that pyrolysis temperature and atmosphere significantly influence bio-oil yield and composition. At a pyrolysis temperature of 500 °C with a heating rate of 7 °C/min, the oil yield was 27.26%. Using nitrogen at a flow rate of 100 $cm^3/min$ as an

inert gas increased the yield by 19.13%. The highest bio-oil yield, 42.12%, was achieved under a steam atmosphere with a steam velocity of 1.3 cm/s. Bio-oils produced under optimal conditions were fractionated into chemical classes using column chromatography. The oil and its subfractions were then analyzed using techniques such as elemental analysis, Proton nuclear magnetic resonance ($^{1}$H-NMR), Fourier-transform infrared spectroscopy (FT-IR), and gas chromatography-mass spectrometry (GC-MS) [16]. French and Czernik evaluated the hydrocarbon production performance of 40 commercial and laboratory-synthesized catalysts through pyrolysis and catalytic cracking. Batch experiments were conducted using three types of biomass feedstocks (cellulose, lignin, and wood) pyrolyzed in quartz boats in direct contact with the catalysts. The process was carried out at temperatures ranging from 400 °C to 600 °C, with catalyst-to-biomass weight ratios of 5:1 to 10:1, to identify the most effective catalysts. The most effective catalysts were from the ZSM-5 group, whereas larger-pore zeolites exhibited lower deoxygenation activity [17]. Kelkar et al. investigated the effects of ten zeolite catalysts on aromatic hydrocarbon production during biomass pyrolysis, using poplar (DN-34) as the feedstock. Analytical pyrolysis with GC/MS revealed that all catalysts, except HZSM-5, produced low levels of aromatics. HZSM-5 was found to be highly effective due to its microporous structure, shape selectivity, and acidity, enabling it to produce aromatics from biomass at moderate temperatures, low pressure, and without the need for molecular hydrogen. Additionally, the silica-to-alumina ratio in HZSM-5 significantly influenced the yield and distribution of aromatic products [18].

In addition to its environmental benefits, biomass pyrolysis also holds significant economic potential. Countries with agriculture-driven economies can greatly benefit from this technology, as large quantities of agricultural residues can be transformed into valuable bio-products. This not only mitigates waste management issues but also opens up revenue-generating opportunities for rural communities. Moreover, the utilization of biomass aligns with global efforts to reduce carbon footprints and transition toward renewable energy systems, further emphasizing its relevance in addressing climate change challenges. This research focused on using grape seeds as a raw material to generate bio-oil and bio-char through the process of pyrolysis. The experiments were carried out under a nitrogen atmosphere at temperatures between 500 and 800 °C. To examine the effects of catalysts on product distribution and composition, catalytic studies were carried out based on the optimal conditions identified during the temperature experiments. The bio-oils and bio-chars were analyzed using various techniques, including GC-MS, FT-IR, and scanning electron microscopy (SEM). Although GC is a widely used technique for detecting volatile substances in organic liquids, it has a limitation of identifying only about 40% of the components in conventional pyrolysis oils. As such, complementary analytical methods were employed for a comprehensive evaluation of the pyrolysis products [19].

This study focused on utilizing grape seeds as a raw material. Grapes are widely consumed, and their seeds are often discarded as waste. Repurposing grape seed waste offers a sustainable solution, both economically and environmentally. Large volumes of grape seed waste generated during wine, fruit juice, and vinegar production can be transformed into valuable products or used for energy production. Grape seeds can be converted into solid, liquid, and gaseous fuels through pyrolysis. This study aimed to enhance the yields and quality of bio-oil and bio-char derived from grape seed pyrolysis through catalytic methods. For the first time, a comparative catalytic pyrolysis experiment was conducted using Purmol CTX and Clinoptilolite, evaluating their effects on product yields and the properties of bio-oils and bio-chars. The availability and low cost of these catalysts provide economic benefits for the pyrolysis process. While the catalysts had a limited impact on product yields, they significantly influenced the composition of bio-oils and the morphology of bio-chars. These findings indicate that the performance of these catalysts could be improved through advanced modification techniques in future research. The products of grape seed pyrolysis have diverse applications. Bio-oil can be used as a liquid fuel in boilers or as a source for alternative chemical production. The gas product, or syngas, can be utilized as renewable energy in heating systems, and bio-char can serve as activated carbon in water treatment or as electrode material in supercapacitors. This study highlights the potential of grape seed pyrolysis as an environmentally friendly and economically viable approach to waste valorization. Finally, this study not only contributes to the existing literature on biomass pyrolysis but also offers practical insights for optimizing product yields and improving their quality. These findings could pave

the way for industrial-scale applications, promoting the use of biomass as a sustainable energy source and advancing global energy transitions.

# II. MATERIALS and METHODS

## A. RAW MATERIAL

Grape seeds, sourced from a local market in Karabük, were used as the primary biomass material. Prior to the experiments, the seeds were milled to obtain a particle size smaller than 0.45 mm. The determinations of moisture, ash, and volatile matter were performed according to ASTM standards [20, 21, 22]. The fixed carbon content was calculated by difference, as indicated in the table 1. The amounts of holocellulose, α-cellulose, and lignin were determined using the methods employed by Teramoto and colleagues [23]. The properties of this biomass are summarized in Table 1.

***Table 1.*** *Properties of grape seed.*

| | | |
|---|---|---|
| **Proximate analysis** *(wt. %)* | Moisture | 7.62 |
| | Volatile matter | 77.51 |
| | Fixed carbon[a] | 11.10 |
| | Ash | 3.77 |
| **Ultimate analysis** *(wt. %)* | C | 51.15 |
| | H | 7.63 |
| | N | 1.75 |
| | O[b] | 39.48 |
| | HHV *(MJ/kg)* | 21.13 |
| **Component analysis** *(wt. %)* | Extractives | 14.14 |
| | α-cellulose | 17.93 |
| | Holocellulose | 43.89 |
| | Lignin | 64.22 |

[a] by difference [100 - (Moisture (%) + Volatile matter (%) + Ash (%)]

[b] by difference [100 - (C (%) + H (%) + N (%)]

HHV: Higher heating value

In this study, the components, degradation temperatures, and catalytic effects of grape seeds were examined. TG-DTA analysis was performed by taking a 10 mg sample (scale sensitivity ± 0.02%) with a nitrogen flow rate of 20 mL/min and a heating rate of 10 °C/min. The TGA spectrum of grape seeds is presented in Figure 1, and the range of 100–250 °C is defined as the region where highly volatile components and moisture are removed, while the region between 250 and 450 °C indicates the degradation of hemicellulose and cellulose. The region after 450 °C, where the mass loss slows down, is indicated as the lignin degradation region. Degradation continues between 450 °C and 800 °C, but at a slow rate. The degradation temperatures of biomass components are quite different from each other and are important for product composition. As a result, the thermal degradation behavior of biomass, which consists of different compounds in varying compositions, also differs. In the thermal analysis of grape seeds, the majority of the degradation occurred below 600 °C. Based on these results, experiments were carried out at 500°C, 600°C, 700°C, and 800°C, with 600°C identified as the optimal temperature.

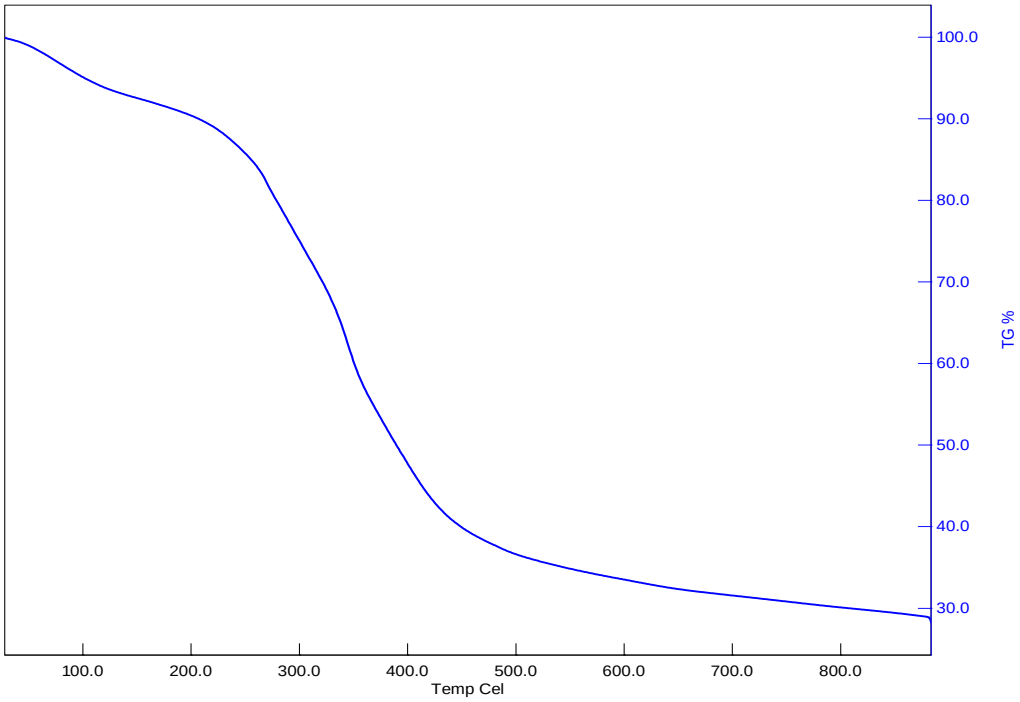


***Figure 1.*** *TGA curves of grape seed.*

## B. CATALYSTS

Two types of catalysts were employed in this study: clinoptilolite, a natural zeolite obtained from Gördes Zeolite Mining (Bayraklı/İzmir), and Purmol CTX, procured from Damlanem Chemistry (Sincan/Ankara). Purmol CTX is a commercially available synthesized catalyst, while clinoptilolite is a naturally occurring zeolite mineral that is widely found in our country. For these reasons, a comparison of the two catalysts was conducted. The chemical compositions of these catalysts, determined using X-ray Fluorescence Spectroscopy (XRF) analysis, are presented in Table 2. The surface morphologies were examined using SEM, with the results presented in Figure 2.

***Table 2****. XRF results of the catalysts.*

| **Catalyst** | **Element** | **Amount** *(wt. %)* |
|---|---|---|
| Clinoptilolite | Si | 80.93 |
| | Al | 6.62 |
| | K | 5.51 |
| | Ca | 3.50 |
| | Fe | 2.32 |
| | Mg | 0.66 |
| Purmol CTX | Si | 66.01 |
| | Al | 22.25 |
| | Na | 9.89 |
| | Ca | 1.05 |
| | K | 0.64 |

Si (Silicium), Al (Aluminum), K (Potassium), Ca (Calcium), Fe (Iron), Mg (Magnesium), Na (Sodium)

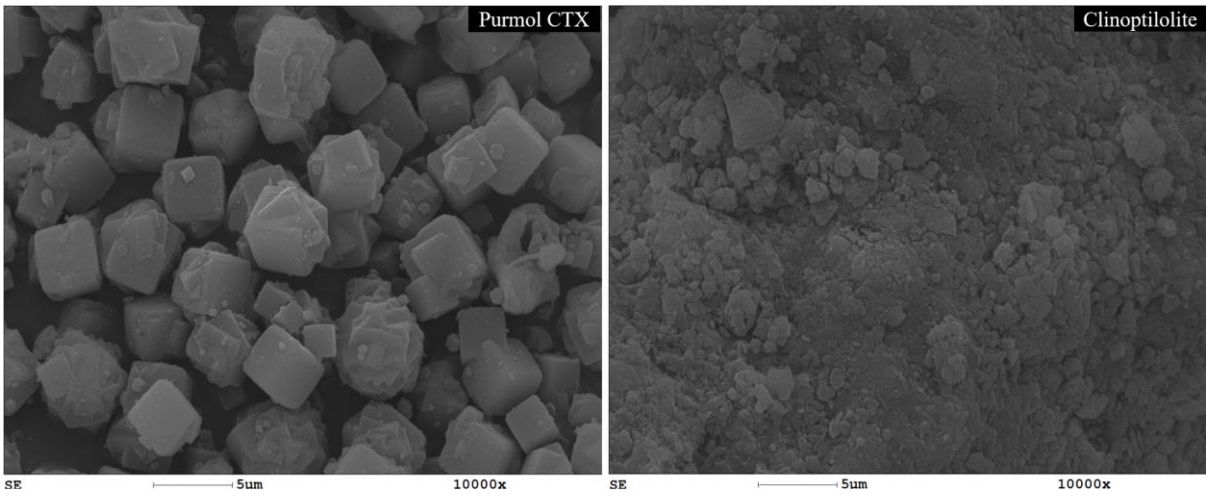


***Figure 2.*** *SEM image of the catalysts.*

## C. EXPERIMENTAL STUDIES

The pyrolysis process was executed using a fixed-bed stainless-steel reactor, which measured 21 cm in height and 6 cm in diameter. Experiments were performed at four distinct temperatures (500, 600, 700, and 800 °C) for a duration of one hour under a nitrogen atmosphere. The experimental setup is illustrated in Figure 3. Approximately 25 grams of dried grape seed waste was loaded into the reactor, which was heated at a controlled rate of 7 °C per minute until reaching the target temperature. Once this temperature was achieved, it was held steady for one hour. The pyrolysis resulted in the production of three distinct product types: solid product (bio-char), liquid product, and gaseous product (bio-gas). The liquid products were collected using three sequential glass condensers: the first two were cooled with a water-ice mixture, while the third was water-cooled. The purpose of this cooling process is to maximize the collection of liquid in the cooling flasks. The liquid product obtained from the pyrolysis of biomass was subjected to liquid-liquid extraction using dichloromethane (DCM) to recover biofuels for analysis and to remove water that might originate from the biomass. The remaining DCM extract after extraction was referred to as bio-oil. The yields of liquid product, bio-char, and DCM extract (bio-oil) were calculated based on mass conservation, with gas yield determined by subtracting the bio-char and liquid yields from 100%.

$$Solid\ product\ yield\ (wt.\%) = \frac{weight\ of\ the\ solid\ product\ (g)}{weight\ of\ raw\ materials\ on\ a\ dry\ basis\ (g)} x100$$

$$Liquid\ product\ yield\ (wt.\%) = \frac{weight\ of\ the\ liquid\ product\ (g)}{weight\ of\ raw\ materials\ on\ a\ dry\ basis\ (g)} x100$$

$$Bio-oil\ yield\ (wt.\%) = \frac{weight\ of\ the\ bio-oil\ (g)}{weight\ of\ raw\ materials\ on\ a\ dry\ basis\ (g)} x100$$

$$Gas\ product\ yield\ (wt.\%) = 100 - (liquid\ product + solid\ product)$$

Catalyst-based experiments were conducted at 600 °C, the temperature yielding the highest liquid product output in the thermal experiments. Each catalyst was used at a weight ratio of 20% relative to the 25 grams of dry biomass, with all catalysts meeting analytical-grade purity standards.

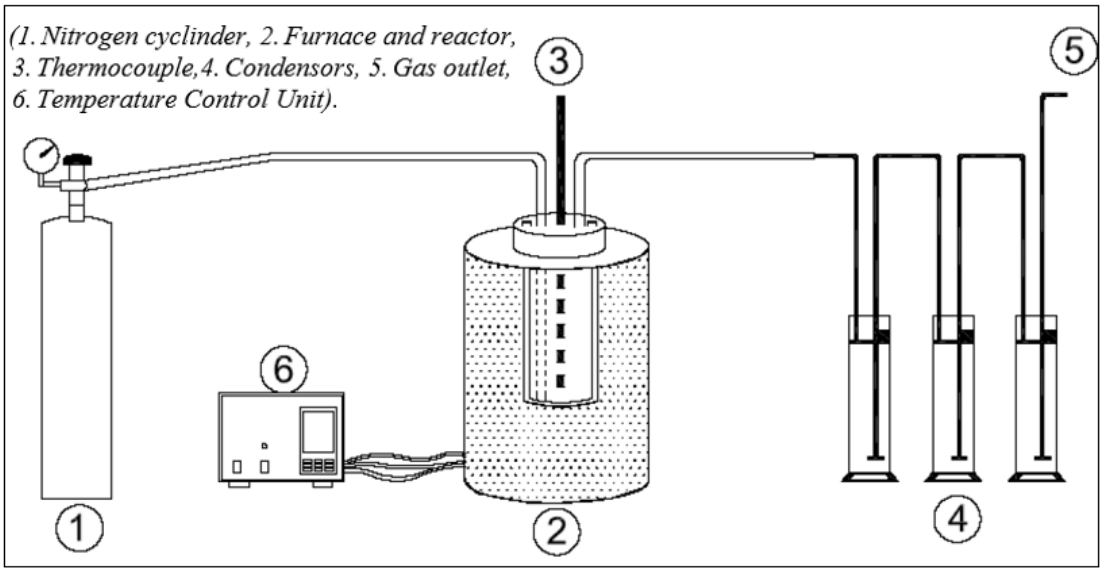


***Figure 3.*** *Pyrolysis system schematic [8].*

### D. ANALYSIS of PYROLYSIS PRODUCTS

The liquid products were extracted using 200 mL of DCM, dried with anhydrous sodium sulfate to remove residual water, and filtered before solvent removal via rotary evaporation. The bio-oil produced from both catalytic and non-catalytic pyrolysis experiments was analyzed by GC-MS. An HP-5MS device, equipped with a 6890 Gas Chromatograph and a phenyl methyl siloxane capillary column, was utilized. Helium, flowing at 1 mL/min, was used as the carrier gas. The injector temperature was held at 250 °C. The GC oven temperature was programmed as follows: initially set to 40 °C and held for 10 minutes, then increased to 170 °C at a rate of 2 °C/min and held for 5 minutes. It was then raised to 250 °C at a rate of 8 °C/min and held for 15 minutes, followed by an increase to 300 °C at a rate of 15 °C/min, where it was held for a final 10 minutes. The GC-MS technique enabled the identification and quantification of volatile organic compounds in the bio-oil, providing crucial information about its chemical composition. The FT-IR (Perkin Elmer FT-IR 100) analysis allowed the determination of key functional groups, helping to characterize the chemical structure of both bio-oils and biochars. The elemental composition of the bio-oil and bio-char was determined using a LECO CHNS 932 analyzer. The higher heating values (HHVs) of biomass, biochars, and bio-oils were calculated using the Dulong formula. SEM (FEI Quanta 450 FEG) was utilized to examine the surface morphology of biochars and raw materials. Additionally, the SEM images provided valuable insight into the structural changes in biochars post-pyrolysis, such as pore formation and surface texture evolution at different pyrolysis temperatures.

## III. RESULTS and DISCUSSION

As shown in Figure 4, the distribution of products obtained from the pyrolysis of grape seeds varies with temperature. As the pyrolysis temperature increased, bio-char yields decreased from 37.7% to 28.7% by weight, while gas yields rose from 15.4% to 30.2%. The maximum bio-char yield was observed at 500 °C. Conversely, the highest yields of liquid products (49.1%) and bio-oil (14.8%) were achieved at 600 °C. However, further increases in temperature led to a decline in liquid and bio-oil yields, attributed to the secondary decomposition of volatile components at elevated temperatures [24]. Catalytic experiments were carried out at 600 °C, the optimal temperature determined from non-catalytic pyrolysis. Figure 5 illustrates the effects of Purmol CTX and clinoptilolite catalysts on the products obtained from the pyrolysis of biomass. Both Purmol CTX and clinoptilolite catalysts reduced the yields of liquid products, bio-char, and bio-oil compared to the non-catalytic conditions, while increasing the

gas product yield. Although the catalysts had minimal impact on overall yields, they significantly altered product composition, highlighting the role of catalysis in modifying pyrolysis outputs.

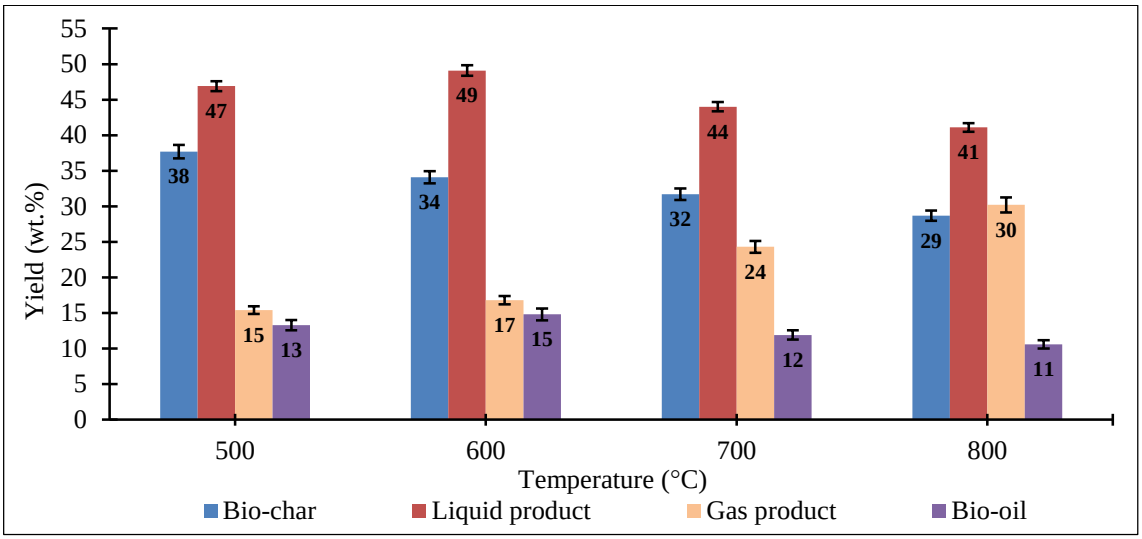


***Figure 4.*** *Distribution of products obtained from experiments at different temperatures (t=60 min).*

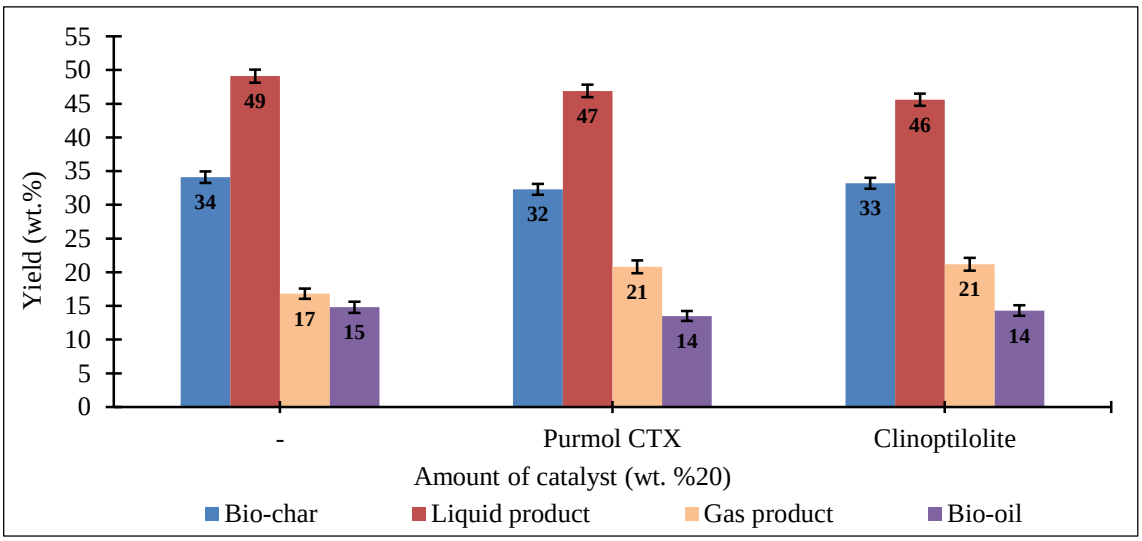


***Figure 5***. *Distribution of products obtained from experiments with and without a catalyst. (T=600 °C, t=60 min).*

The elemental compositions and heating values of the bio-chars and bio-oils derived from grape seed pyrolysis are shown in Tables 3 and 4, respectively. Bio-chars exhibit higher carbon content and lower oxygen content compared to the raw material. The H/C atomic ratios of the biochars decrease as the pyrolysis temperature increases, with the lowest H/C ratio observed at the highest pyrolysis temperature. These results indicate a higher presence of aromatic compounds in the biochars. The heating value is a critical factor affecting the quality of biochars, and it was observed to increase compared to the raw material. Because the oxygen, which is present in high amounts in biomass and causes a decrease in thermal value, has been removed from the structure after the pyrolysis process. The highest higher heating value (HHV) was achieved at 600 °C. Elemental analysis of the liquid products shows that, compared to the raw material, the carbon content and heating value decreased while the oxygen content increased. The increase in oxygen content, as supported by GC-MS results, indicates a rise in acidic products. The highest carbon content and heating value for liquid products were recorded at 700 °C. The increase in the H/C ratio compared to the raw material suggests a reduction in aromatic structures in the liquid products. The percentages of carbon recovered in biochars and bio-oils obtained from the pyrolysis processes were calculated and are shown in Table 5. For non-catalytic experiments, the

percentage of recovered carbon in biochars was higher than in bio-oils. As the temperature increased, the percentage of carbon recovered in biochars decreased. Examining the total recovered carbon, higher values were observed at lower temperatures.

***Table 3.*** *The elemental composition of bio-chars (t=60 min.)*

| **Temperature** *(°C)* | **C** | **H** | **N** | **O[a]** | **H/C[b]** | **O/C[b]** | **N/C[b]** | **HHV[c]** *(MJ/kg)* |
|---|---|---|---|---|---|---|---|---|
| Raw Material | 51.15 | 7.63 | 1.75 | 39.48 | 1.79 | 0.58 | 0.029 | 21.13 |
| 500 | 75.85 | 4.04 | 2.89 | 17.22 | 0.64 | 0.17 | 0.033 | 28.33 |
| 600 | 79.84 | 3.00 | 2.60 | 14.56 | 0.45 | 0.14 | 0.028 | 28.67 |
| 700 | 80.67 | 2.17 | 2.34 | 14.82 | 0.32 | 0.14 | 0.025 | 27.72 |
| 800 | 81.55 | 1.81 | 2.14 | 14.50 | 0.27 | 0.13 | 0.023 | 27.56 |

[a] by difference
[b] atomic ratio
[c] Higher heating value *(HHV)*

***Tablo 4.*** *The elemental composition of bio-oils (t=60 min.)*

| **Temperature** *(°C)* | **C** | **H** | **N** | **O[a]** | **H/C[b]** | **O/C[b]** | **N/C[b]** | **HHV[c]** *(MJ/kg)* |
|---|---|---|---|---|---|---|---|---|
| Raw Material | 51.15 | 7.63 | 1.75 | 39.48 | 1.79 | 0.58 | 0.029 | 21.13 |
| 500 | 38.18 | 9.46 | 1.72 | 50.64 | 2.97 | 0.99 | 0.039 | 17.37 |
| 600 | 40.17 | 7.57 | 2.02 | 50.24 | 2.26 | 0.94 | 0.043 | 15.42 |
| 700 | 47.30 | 8.74 | 2.25 | 41.72 | 2.22 | 0.66 | 0.041 | 21.02 |
| 800 | 42.13 | 7.59 | 2.46 | 47.83 | 2.16 | 0.85 | 0.050 | 16.54 |

[a] by difference
[b] atomic ratio
[c] Higher heating value *(HHV)*

***Table 5.*** *Carbon recovery (t = 60 min).*

| **Temperature** *(°C)* | **Carbon Recovered in Crude Bio-Oils** *(wt. %)* | **Carbon Recovered in Solid Residues** *(wt. %)* | **Total Carbon Recovered** *(wt. %)* |
|---|---|---|---|
| 500 | 9.93 | 55.90 | 65.83 |
| 600 | 11.62 | 53.23 | 64.85 |
| 700 | 11.00 | 50.00 | 61.00 |
| 800 | 8.73 | 45.76 | 54.49 |

The functional group analysis of biochars produced from grape seed pyrolysis at various temperatures is presented in Figure 6. The biochars exhibited similar functional groups, which diminished as the pyrolysis temperature increased. At 500 °C, distinct functional groups were identified, including peaks at 2,918 and 2,853 $cm^{-1}$, corresponding to aliphatic C-H stretching vibrations; peaks at 1,407 and 1,555 $cm^{-1}$, confirming aromatic C=C stretching vibrations of aromatic rings; and a peak at 1,035 $cm^{-1}$, indicative of C-H out-of-plane bending vibrations. These peaks were prominent at 500 °C but degraded at higher temperatures (600, 700, and 800 °C). Additionally, prominent aliphatic C-H stretching vibrations at 2,855 and 2,924 $cm^{-1}$ and an aromatic carbonyl C=O peak at 1,743 $cm^{-1}$, which were evident in the raw material, disappeared in the biochars as the temperature increased, reflecting the breakdown of biomass structures during pyrolysis. In the catalytic experiments shown in Figure 7, the FT-IR spectra of the biochars exhibited a broad, significant peak at 1,000 $cm^{-1}$, attributed to catalyst residues, which was further validated by SEM-EDS and XRF analyses.

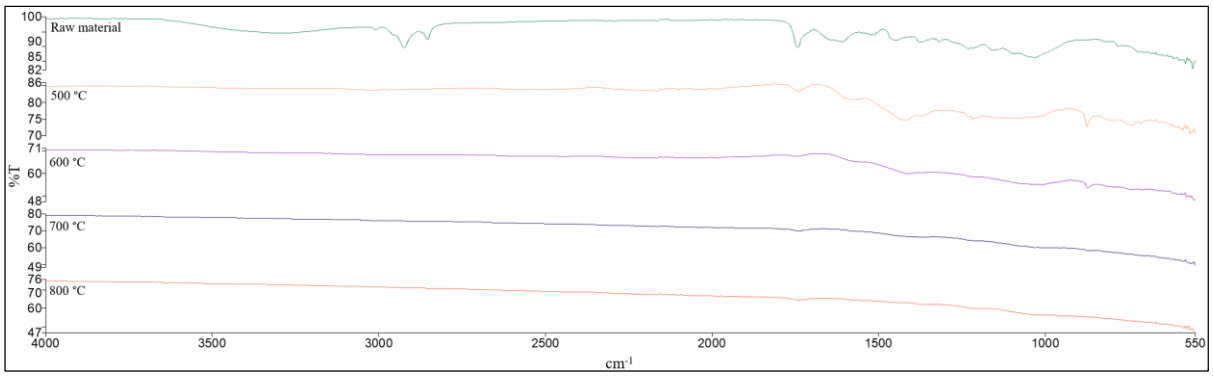


***Figure 6.*** *FT-IR results of bio-char at different temperatures (500, 600, 700, and 800 °C).*

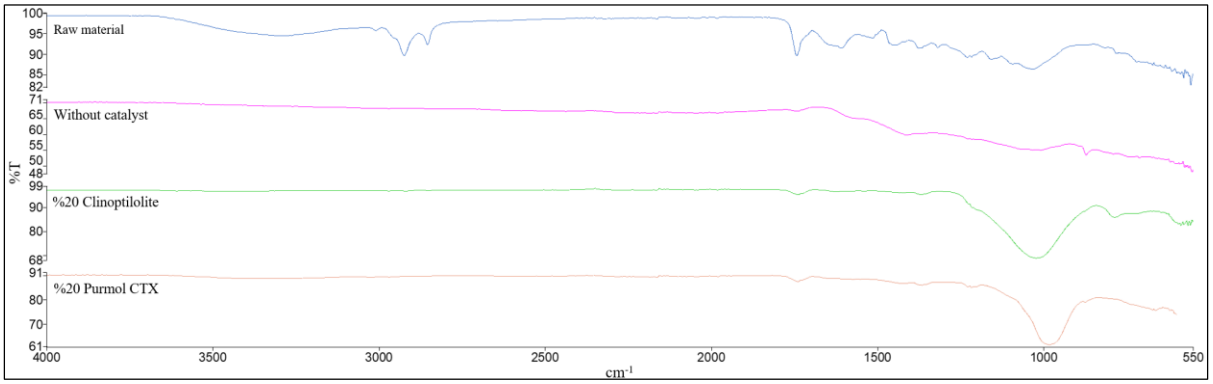


***Figure 7.*** *FT-IR results of bio-char at 600 °C with and without a catalyst.*

Figure 8 illustrates the FT-IR spectra of bio-oils derived from grape seed pyrolysis alongside spectra of the raw materials. A broad band between 3,200 and 3,600 $cm^{-1}$ indicates the presence of OH groups. Peaks at 2,855 and 2,924 $cm^{-1}$ confirm aliphatic C-H stretching vibrations, while peaks at 1,709 and 1,743 $cm^{-1}$ represent aromatic carbonyl C=O groups. Peaks between 1,100 and 1,200 $cm^{-1}$ correspond to C-O stretching vibrations, and the peak at 1,035 $cm^{-1}$ is indicative of C-H out-of-plane bending vibrations in alkene groups. Peaks between 680 and 900 $cm^{-1}$ are associated with benzene rings. Figure 9 compares FT-IR spectra of bio-oils from catalytic and non-catalytic pyrolysis as well as the raw material, showing similar results across conditions. The analysis of biochar and bio-oil functional groups reveals several critical insights into the pyrolysis process and its optimization. The degradation of functional groups, particularly at elevated temperatures, emphasizes the role of temperature in controlling the product's chemical composition. The disappearance of oxygenated groups, such as C-H and C=O bonds, aligns with the increasing carbon content and stability of biochar, which can be used as a solid fuel or as a carbon sequestration agent.

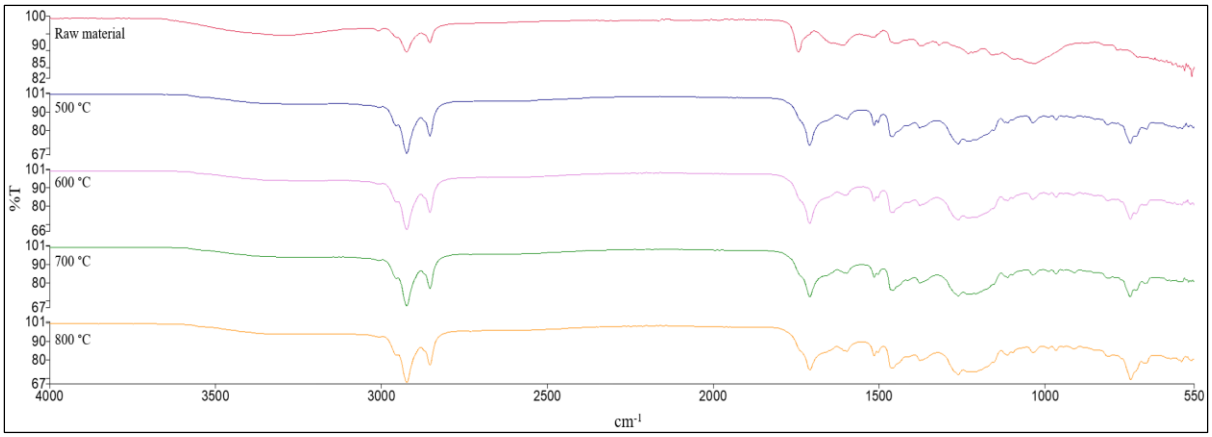


***Figure 8.*** *FT-IR results of bio-oil at different temperatures (500, 600, 700, and 800 °C).*

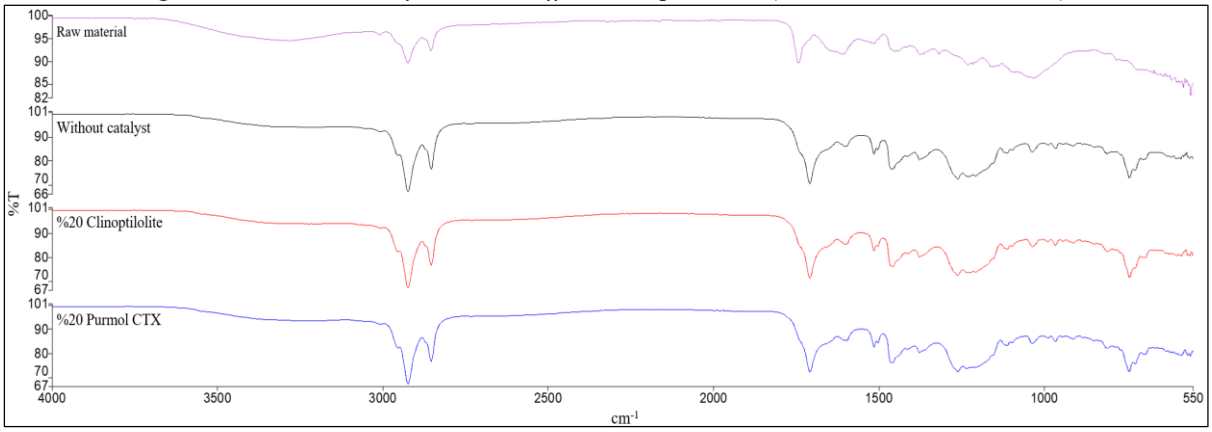


***Figure 9.*** *FT-IR results of bio-oils at 600 °C with and without a catalyst.*

The SEM images of grape seeds and the biochars obtained from pyrolysis at various temperatures are shown in Figure 10. SEM analysis revealed significant structural changes in biochars following thermal treatment. These images provide valuable insights into pore structure and surface morphology changes during carbonization [25]. From the SEM micrographs, it is evident that the physical properties and surface morphology of the biomass samples change after the pyrolysis process. The raw grape seed samples exhibit a smooth surface morphology with minimal porosity, indicative of their unaltered structure. However, with the onset of pyrolysis, significant changes in surface characteristics are observed, highlighting the impact of thermal decomposition on the material. The surfaces of the biochars change with increasing temperature compared to the raw material. As known, higher volatile matter release results in biochars with lower density, higher porosity, and significantly different pore structures [26]. In the biochars obtained from grape seeds, pore formation is clearly visible at 500 °C due to the volatilization of the components in the biomass. At 600 °C and 700 °C, the pores become smaller. This indicates the progressive transformation of biomass into a more carbon-rich material, accompanied by the compaction of the structure due to the thermal decomposition of lignin, cellulose, and hemicellulose. As the temperature increases, it is thought that the volatile contents of the lignin fractions close the pores. With the temperature rising to 800 °C, a reduction in pores is observed, and carbon spheres replace them. The formation of carbon spheres is attributed to the deposition and rearrangement of carbon-rich residues during the final stages of pyrolysis, suggesting a more graphitic or ordered structure in the biochar matrix. The SEM images of the biochars obtained from the pyrolysis of raw materials in both catalytic and non-catalytic environments at 600 °C are presented in Figure 11. When examining the SEM images, the pores formed in the biochar obtained at 600 °C stand out compared to the raw material. However, it is observed that the pores are closed with the use of both catalysts. This pore-closing effect is primarily due to the interaction between the catalysts and the pyrolysis vapors, which promotes secondary reactions and residue deposition within the pore structure. Moreover, the catalytic environment is likely to facilitate the decomposition of certain biomass components, leading to structural

compaction. According to the elemental composition analysis of the scanning electron microscope (SEM-EDS) shown in Figure 12, the pores are seen to be filled by catalyst residues. This finding underscores the significant role of catalysts in altering not only the chemical composition but also the physical attributes of biochars. The incorporation of catalysts such as Purmol CTX and Clinoptilolite introduces new surface features and potentially enhances the biochar's application-specific properties, such as adsorption capacity or thermal stability.

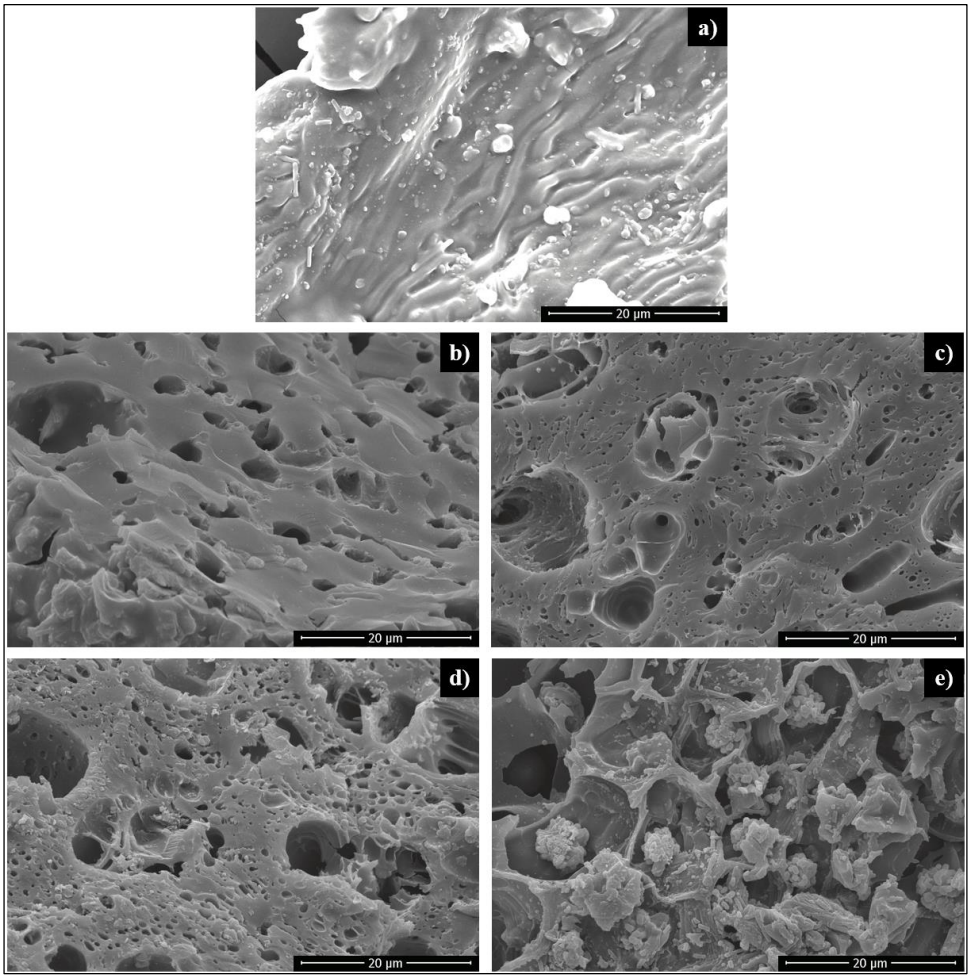


***Figure 10.*** *SEM images of raw grape seeds and bio-chars obtained from the pyrolysis of grape seeds at different temperatures (t = 60 min)*
*a) raw material, b) 500 °C, c) 600 °C, d) 700 °C, e) 800 °C*

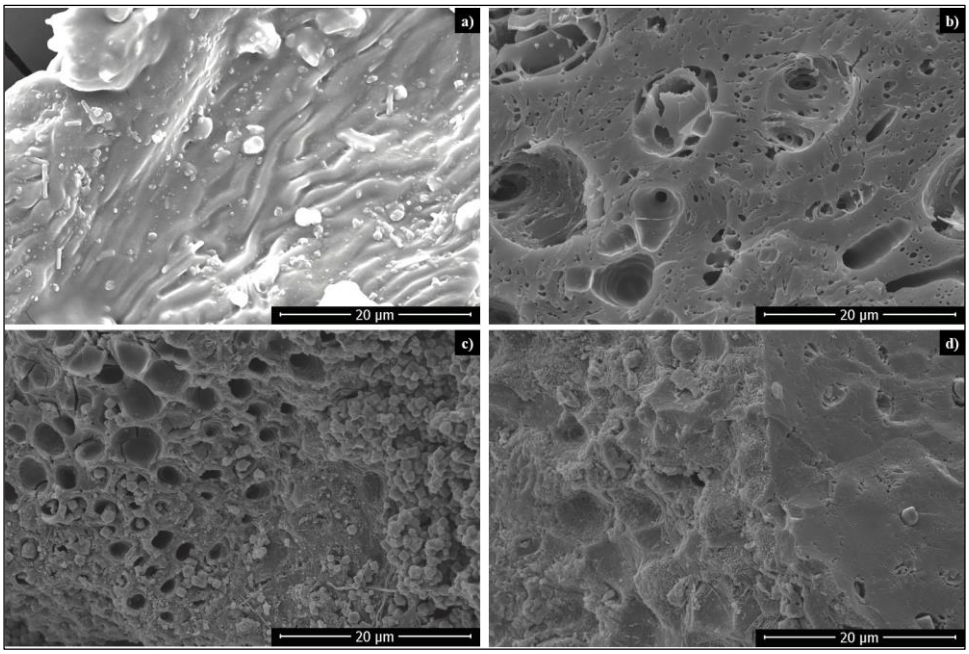


***Figure 11.*** *SEM images of raw grape seeds and bio-chars obtained from the pyrolysis process at 600 °C with and without a catalyst (t = 60 min).*
*a) raw material, b) without catalyst, c) wt. %20 Purmol CTX, d) wt. %20 Clinoptilolite*

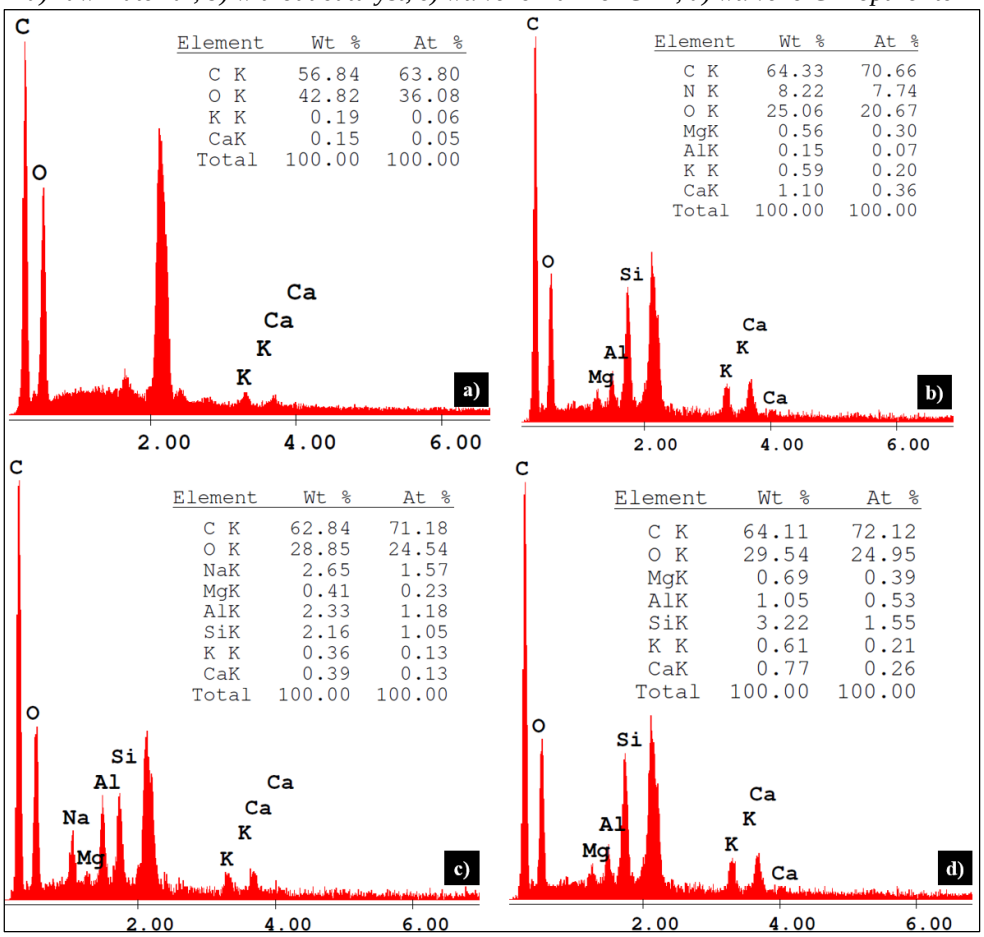


***Figure 12.*** *EDS analysis of raw grape seeds and bio-chars obtained from the pyrolysis process at 600 °C with and without a catalyst (t = 60 min).*
***a)*** *raw material,* ***b)*** *without catalyst****, c)*** *wt. %20 Purmol CTX,* ***d)*** *wt. %20 Clinoptilolite*

The GC-MS analysis of bio-oils derived from grape seed pyrolysis under both catalytic and non-catalytic conditions is summarized in Table 6. The chemical composition of the bio-oils was predominantly characterized by oxygenated compounds, including phenol, 2-methoxyphenol, 4-methylphenol, 2-methoxy-4-methylphenol, 4-ethyl-2-methoxyphenol, and several fatty acids such as n-hexadecanoic acid, (Z,Z)-9,12-octadecadienoic acid, and octadecanoic acid. Catalytic pyrolysis significantly influenced the bio-oil composition, resulting in increased levels of acidic compounds compared to non-catalytic conditions, as depicted in Figure 13. Table 6 provides a detailed breakdown of the chemical compounds identified in the bio-oils under different conditions at 600 °C and a reaction time of 60 minutes. Compounds such as 2-methoxyphenol and 4-methylphenol, known for their applications in chemical industries, were observed in higher proportions in catalytic experiments, particularly when Purmol CTX and clinoptilolite were used as catalysts. Interestingly, the use of Purmol CTX resulted in a higher production of phenols, while clinoptilolite exhibited a relatively balanced effect on a broader range of compounds. Figure 13 categorizes the identified chemical compounds, highlighting their diverse chemical nature. Phenolic compounds, alkenes, aromatic hydrocarbons, and fatty acid derivatives formed the majority of the bio-oil composition. For example, 9-eicosyne, a long-chain alkene, was abundant in non-catalytic conditions but decreased significantly in catalytic pyrolysis. Conversely, fatty acids such as (E)-9-octadecenoic acid increased drastically under catalytic conditions, indicating enhanced breakdown and conversion of biomass-derived intermediates. The differences in chemical compositions between catalytic and non-catalytic pyrolysis underline the pivotal role of catalysts in determining product specificity. Zeolite catalysts play a crucial role in deoxygenation reactions, enabling the conversion of oxygenated compounds found in bio-oil into lighter hydrocarbons [27]. These catalysts facilitate the cracking of heavy organic molecules and support aromatization reactions, transforming aliphatic hydrocarbons into aromatic compounds [28]. Their porous structure and acidic properties are particularly effective in promoting isomerization reactions, where carbon chains are rearranged [29]. Furthermore, zeolite catalysts contribute to carbonization reactions, regulating the carbon structure and aiding in the production of porous bio-char [30]. Phenolic compounds are essential for industrial applications, such as the production of resins and adhesives. The increased presence of phenolic derivatives in catalytic pyrolysis indicates promising opportunities for upgrading bio-oils into value-added products. The substantial presence of fatty acids such as (Z,Z)-9,12-octadecadienoic acid and their methyl esters in both catalytic and non-catalytic conditions indicates the suitability of grape seed pyrolysis for biofuel applications. Catalytic processes, however, enhance the formation of these compounds, making the oil more energy-dense and viable for biofuel production. Hydrocarbons and alkenes, such as long-chain alkenes like 1-hexadecene and 9-eicosyne found under non-catalytic conditions, were partially replaced by shorter chains and aromatic compounds in catalytic environments, indicating a catalyst-driven shift in reaction pathways. Overall, the catalytic experiments demonstrated an ability to fine-tune the bio-oil composition toward specific applications, enhancing the potential for industrial utility. However, the presence of certain nitrogen-containing compounds, such as hexadecanenitrile, highlights the need for further refinement to reduce impurities and improve bio-oil quality. Future studies can explore the influence of different catalyst types and concentrations to further refine the pyrolysis process, enhancing both bio-oil quality and biochar yield. Additionally, a deeper investigation into the mechanisms of catalytic pyrolysis could help optimize the degradation pathways and provide a more comprehensive understanding of how catalysts impact product distribution.

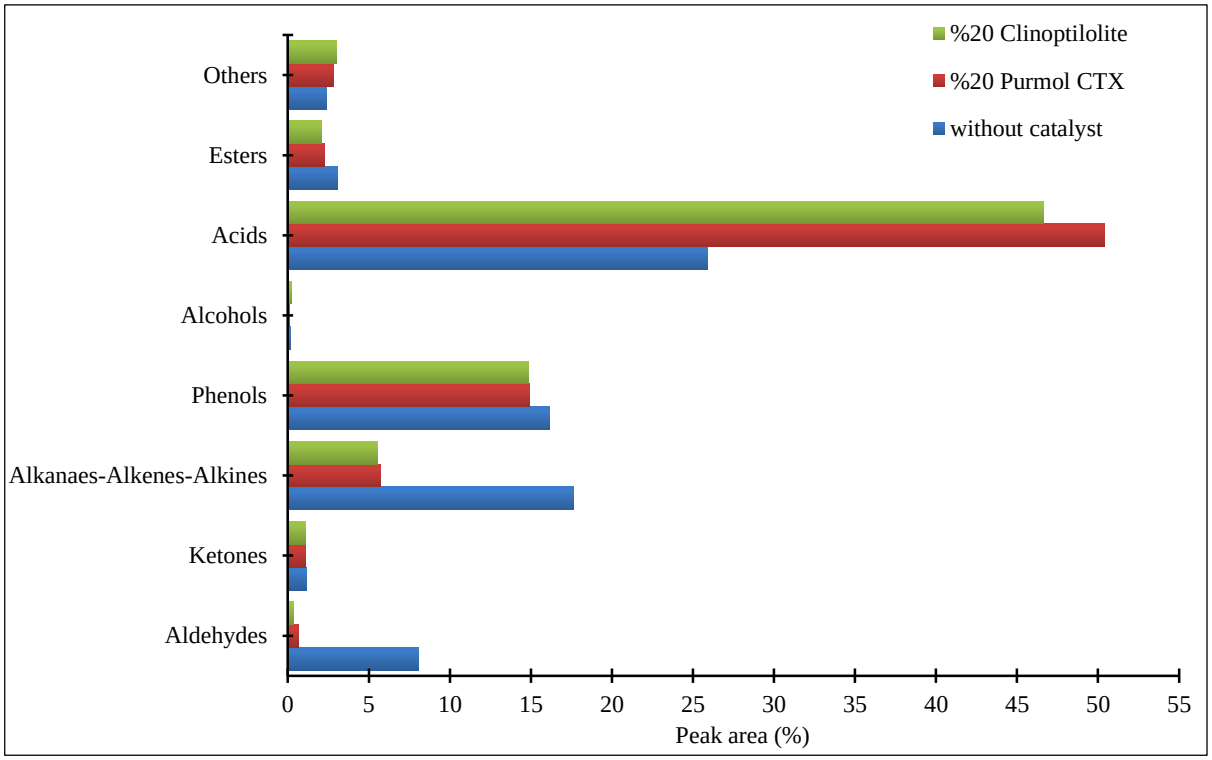


***Figure 13.*** *Classification of the chemical compounds identified in the bio-oils obtained from the pyrolysis of grape seeds in non-catalytic and catalytic environments (T=600 °C, t=60 min).*

***Table 6****. Identified chemical compounds in the bio-oils obtained from the pyrolysis of grape seeds in non-catalytic and catalytic environments (T = 600 °C, t = 60 min).*

| **Retention time (min)** | **Compounds** | **Peak area** *(%)* | | |
|---|---|---|---|---|
| | | - | **Purmol CTX** *(wt. %20)* | **Clinoptilolite** *(wt. %20)* |
| 3.26 | Propanoic acid | 0.21 | 0.10 | 0.09 |
| 4.00 | Toluene | 0.24 | 0.19 | 0.16 |
| 8.39 | 1,3-Dimethylbenzene | 0.48 | - | - |
| 8.41 | 1,2-Dimethylbenzene | - | 0.37 | 0.34 |
| 9.88 | p-Xylene | - | - | 0.27 |
| 11.20 | 2-Methyl-2-cyclopenten-1-one | 0.24 | 0.22 | 0.24 |
| 12.01 | Butyrolactone | 0.22 | - | 0.20 |
| 20.03 | 1-Decene | 0.28 | 0.28 | 0.29 |
| 21.29 | Phenol | **1.05** | **1.36** | **1.21** |
| 24.23 | Indene | - | 0.42 | 0.33 |
| 25.72 | Butylbenzene | 0.27 | 0.25 | 0.24 |
| 27.59 | 2-Methylphenol | 0.55 | 0.61 | 0.72 |
| 29.21 | 2-Methoxyphenol | **3.90** | **3.14** | **3.04** |
| 29.37 | 1-Undecene | 0.27 | 0.27 | 0.29 |
| 29.49 | 4-Methylphenol | **1.01** | **1.66** | **1.83** |
| 34.24 | Pentylbenzene | 0.46 | 0.45 | 0.47 |
| 34.93 | 2,3-Dimethylphenol | 0.60 | 0.19 | 0.50 |
| 34.94 | 2,4-Dimethylphenol | - | 0.45 | - |
| 35.64 | Naphthalene | 0.36 | 0.33 | 0.28 |
| 36.13 | 2-Methoxy-4-methylphenol | **2.94** | **2.36** | **2.30** |
| 36.14 | 1,4-Dimethoxybenzene | - | 0.47 | - |
| 36.61 | 4-Ethylphenol | 0.15 | 0.42 | 0.47 |
| 36.77 | 3,5-Dimethylphenol | 0.48 | - | - |
| 36.78 | 2,3-Dimethylphenol | - | 0.62 | 0.72 |
| 38.92 | Octanoic Acid | 0.32 | - | 0.08 |
| 40.45 | 1,2-Benzenediol | 0.47 | 0.18 | 0.46 |
| 41.03 | 3,4-Dimethoxytoluene | 0.29 | - | 0.29 |
| 43.52 | 4-Eethyl-2-methoxyphenol | **2.42** | **2.10** | **1.89** |
| 43.64 | 2-Methylnaphthalene | 0.19 | 0.25 | 0.21 |
| 44.43 | 1-Tridecene | 0.23 | 0.24 | 0.24 |
| 44.99 | Tridecene | 0.23 | 0.21 | 0.19 |
| 45.83 | 2-Methoxy-4-vinylphenol | 0.25 | 0.23 | 0.23 |
| 46.39 | 4-Methyl-1,2-benzenediol | 0.17 | 0.29 | 0.27 |
| 48.74 | 2-Methoxy-3-(2-propenyl)phenol | 0.61 | - | - |
| 49.32 | 2-Methoxy-4-propylphenol | 0.72 | 0.57 | 0.51 |
| 51.00 | (E)-2-Tetradecene | 0.45 | 0.50 | - |

| | | | | |
|---|---|---|---|---|
| 51.02 | 1-Tetradecene | - | - | 0.51 |
| 51.51 | Tetradecene | 0.19 | 0.23 | 0.25 |
| 54.51 | 2-Methoxy-4-(1-propenyl)phenol | 0.84 | 0.67 | 0.64 |
| 56.87 | 1-(4-Hydroxy-3-methoxyphenyl)ethanone | 0.41 | 0.21 | 0.19 |
| 57.14 | 1-Pentadecene | 0.30 | 0.24 | 0.25 |
| 57.62 | Pentadecane | 0.56 | 0.54 | 0.55 |
| 59.52 | 4-Hydroxy-3-methoxybenzeneacetic acid | 0.25 | - | 0.19 |
| 62.45 | Cyclohexadecane | 0.27 | 0.32 | - |
| 62.95 | 1-Hexadecene | - | 0.25 | 0.24 |
| 67.50 | 8-Heptadecene | 0.63 | 0.63 | 0.58 |
| 68.83 | Tetradecane | 0.33 | - | - |
| 68.84 | Heptadecane | - | 0.38 | 0.39 |
| 78.96 | Hexadecanenitrile | 0.19 | 0.32 | 0.34 |
| 80.31 | Hexadecanoic acid methyl ester | 0.60 | 0.50 | 0.46 |
| 83.79 | n-Hexadecanoic acid | **9.07** | **8.48** | **8.44** |
| 88.39 | 1-Hexadecene | 0.27 | - | - |
| 88.51 | Octadecanal | - | 0.51 | - |
| 88.65 | 1-Pentyl-4-(4-propylcyclohexyl)cyclohexene | 0.29 | - | - |
| 88.67 | 1,9-Tetradecadiene | - | 0.26 | 0.24 |
| 89.01 | 9,12-Octadecadienoic acid methyl ester | 0.36 | 0.28 | - |
| 89.04 | 8,11-Octadecadienoic acid methyl ester | - | - | 0.24 |
| 89.28 | 10-Octadecenoic acid methyl ester | 0.61 | - | - |
| 89.30 | 11-Octadecenoic acid methyl ester | - | 0.48 | 0.51 |
| 89.47 | Octadecanenitrile | 0.33 | 0.25 | - |
| 89.49 | Heptadecanenitrile | - | - | 0.27 |
| 89.58 | 10,13-Octadecadienoic acid methyl ester | 0.40 | - | - |
| 89.60 | (Z)-9,17-Octadecadienal | - | - | 0.33 |
| 90.30 | Octadecanoic acid methyl ester | 0.45 | 0.53 | 0.50 |
| 91.32 | (Z,Z)-9,12-Octadecadienoic acid | **10.29** | **6.85** | **6.33** |
| 91.35 | 9-Eicosyne | **12.76** | **-** | **-** |
| 91.53 | (Z)-9,17-Octadecadienal | **7.91** | **-** | **-** |
| 92.02 | (E)-9-Octadecenoic acid | **-** | **29.11** | **25.86** |
| 92.33 | Octadecanoic acid | **5.73** | **5.73** | **5.64** |
| 92.54 | Hexadecanamide | 0.64 | - | 1.20 |
| 92.75 | Dodecanamide | 0.27 | 1.19 | 0.23 |
| 93.93 | 3-Dodecyl-2,5-furandione | 0.62 | - | - |
| 93.98 | 4-Pentyl-1-(4-propylcyclohexyl)cyclohexene | 0.35 | 0.84 | 0.60 |
| 96.19 | (E,E)-9,12-Octadecadienoic acid methyl ester | | 0.29 | 0.27 |
| 96.32 | (Z)-9-Octadecenamide | 0.53 | 0.46 | 0.47 |
| 103.49 | Tetracosane | - | 0.23 | 0.21 |
| 107.88 | Stigmastan-3,5-dien | 0.50 | 0.44 | 0.48 |

# IV. CONCLUSION

Pyrolysis of the biomass sample was conducted at temperatures ranging from 500 to 800 °C, with the outcomes evaluated through catalytic experiments performed under optimal conditions identified in prior thermal studies. The maximum yield of bio-char (37.7%) was obtained at 500°C, while the highest yields of liquid products (49.1%) and bio-oil (14.8%) were achieved at 600°C. Although catalytic studies had a limited effect on the overall yields of bio-oil and bio-char, they significantly influenced the composition of the products. Analysis of elemental composition and heating values revealed that increasing the pyrolysis temperature resulted in higher carbon content and heating values in the bio-chars, alongside a reduction in oxygen content compared to the raw material. The highest higher heating value among the bio-chars, 28.67 MJ/kg, was achieved at 600°C. Among the bio-oils, the highest higher heating value (HHV) of 21.02 MJ/kg was achieved at 700°C. Moreover, the surface structure of the bio-chars exhibited noticeable changes under varying pyrolysis temperatures and catalytic conditions. At higher temperatures, numerous pores of different sizes emerged on the bio-char surfaces derived from grape seeds, while these pores were observed to be filled in the presence of catalysts during catalytic experiments. Additionally, the catalysts significantly altered the morphological structure of the bio-chars compared to the raw material. The influence of the catalysts led to a more homogeneous surface structure in the bio-chars, with noticeable changes in pore sizes and distribution. These modifications enhanced the properties of the bio-chars, making them more suitable for various applications. This research highlights the potential of transforming waste biomass into high-value products, such as bio-oils and bio-chars, underscoring the environmental and economic importance of converting waste biomass into sustainable resources.

# V. REFERENCES


[1] Bensidhom, G., Hassen-Trabelsi, A. B., Alper, K., Sghairoun, M., Zaafouri, K., and Trabelsi, I., "Pyrolysis of Date palm waste in a fixed-bed reactor: Characterization of pyrolytic products," *Bioresource Technology*, vol. 247, pp. 363-369, 2018.

[2] Bonelli, P. R., Della Rocca, P. A., Cerrella, E. G., and Cukierman, A. L., "Effect of pyrolysis temperature on composition, surface properties and thermal degradation rates of Brazil Nut shells," *Bioresource Technology*, vol. 76, no. 1, pp. 15-22, 2001.

[3] Czernik, Stefan, and Anthony V. Bridgwater. "Overview of applications of biomass fast pyrolysis oil." *Energy & Fuels*, vol. 18, no. 2, pp. 590-598, 2004.

[4] Bertero, M., Gorostegui, H. A., Orrabalis, C. J., Guzmán, C. A., Calandri, E. L., and Sedran, U., "Characterization of the liquid products in the pyrolysis of residual chañar and palm fruit biomasses," *Fuel*, vol. 116, pp. 409-414, 2014.

[5] Bridgwater, A. V., "Principles and practice of biomass fast pyrolysis processes for liquids," *Journal of Analytical and Applied Pyrolysis*, vol. 51, no. 1-2, pp. 3-22., 1999.

[6] Bridgwater, Anthony V., D. Meier, and D. Radlein., "An overview of fast pyrolysis of biomass," *Organic Geochemistry*, vol. 30, no. 12, pp. 1479-1493, 1999.

[7] McKendry, Peter., "Energy production from biomass (part 2): conversion technologies," *Bioresource Technology*, vol. 83, no. 1, pp. 47-54, 2002.

[8] Alper, Koray, Kubilay Tekin, and Selhan Karagöz, "Pyrolysis of agricultural residues for bio-oil production," *Clean Technologies and Environmental Policy*, vol. 17, pp. 211-223, 2015.

[9] Demiral, İlknur, and Emine Aslı Ayan, "Pyrolysis of grape bagasse: effect of pyrolysis conditions on the product yields and characterization of the liquid product," *Bioresource Technology*, vol. 102, no. 4, pp. 3946-3951, 2011.

[10] Horne, Patrick A., and Paul T. Williams, "Influence of temperature on the products from the flash pyrolysis of biomass," *Fuel*, vol.75, no. 9, pp. 1051-1059 (1996).

[11] Xu, R., Ferrante, L., Briens, C., and Berruti, F., "Flash pyrolysis of grape residues into biofuel in a bubbling fluid bed," *Journal of Analytical and Applied Pyrolysis*, vol. 86, no.1, pp. 58-65, 2009.

[12] Bridgwater, A. V., and G. V. C. Peacocke., "Fast pyrolysis processes for biomass," *Renewable and Sustainable Energy Reviews*, vol. 4, no. 1, pp. 1-73, 2000.

[13] Wu, L., Guo, S., Wang, C., and Yang, Z., "Production of alkanes (C7-C29) from different part of poplar tree via direct deoxy-liquefaction," *Bioresource Technology*, vol. 100, no. 6, pp. 2069-2076, 2009.

[14] Mackay, D. M., and P. V. Roberts. "The influence of pyrolysis conditions on yield and microporosity of lignocellulosic chars." *Carbon*, vol. 20, no. 2, pp. 95-104, 1982.

[15] Raja, S. A., Kennedy, Z. R., Pillai, B. C., and Lee, C. L. R., "Flash pyrolysis of jatropha oil cake in electrically heated fluidized bed reactor," *Energy*, vol. 35, no. 7, pp. 2819-2823, 2010.

[16] Pütün, A. E., Uzun, B. B., Apaydin, E., and Pütün, E., "Bio-oil from olive oil industry wastes: Pyrolysis of olive residue under different conditions," *Fuel Processing Technology*, vol. 87, no. 1, pp. 25-32, 2005.

[17] French, Richard, and Stefan Czernik., "Catalytic pyrolysis of biomass for biofuels production," *Fuel Processing Technology*, vol. 91, no.1, pp. 25-32, 2010.

[18] Kelkar, S., Saffron, C. M., Andreassi, K., Li, Z., Murkute, A., Miller, D. J., and Kriegel, R. M., "A survey of catalysts for aromatics from fast pyrolysis of biomass," *Applied Catalysis B: Environmental*, vol. 174, pp. 85-95, 2015.

[19] Scholze, B., and D. Meier., "Characterization of the water-insoluble fraction from pyrolysis oil (pyrolytic lignin). Part I. PY-GC/MS, FTIR, and functional groups," *Journal of Analytical and Applied Pyrolysis*, vol. 60, no. 1, pp. 41-54, 2001.

[20] *Standard test method for moisture analysis of particulate wood fuels*, ASTM E871-82, 2006.

[21] *Standard test method for volatile matter in the analysis of particulate wood fuels*, ASTM E872-82, 2006.

[22] *Standard test method for ash in biomass*, ASTM E1755-01, 2007.

[23] Teramoto, Y., Tanaka, N., Lee, S. H., and Endo, T., "Pretreatment of eucalyptus wood chips for enzymatic saccharification using combined sulfuric acid-free ethanol cooking and ball milling," *Biotechnology and Bioengineering*, vol.99, no.1, pp. 75-85, 2008.

[24] Uçar, Suat, and Selhan Karagöz., "The slow pyrolysis of pomegranate seeds: The effect of temperature on the product yields and bio-oil properties," *Journal of Analytical and Applied Pyrolysis*, vol. 84, no. 2, pp. 151-156, 2009.

[25] Özçimen, Didem, and Ayşegül Ersoy-Meriçboyu., "Characterization of biochar and bio-oil samples obtained from carbonization of various biomass materials," *Renewable Energy*, vol. 35, no.6, pp. 1319-1324, 2010.

[26] Haykırı-Açma, Hanzade, Ayşegül Ersoy-Meriçboyu, and Sadriye Küçükbayrak., "Effect of mineral matter on the reactivity of lignite chars," *Energy Conversion and Management*, vol. 42, no. 1, pp. 11-20, 2001.

[27] Sandoval-Rangel, L., Ramírez-Murillo, C. J., Dimas-Rivera, G. L., De La Rosa, J. R., Lucio-Ortiz, C. J., Ahmad, E., and Mendoza, A., "Enhancing the quality of products from slow pyrolysis of an agro-industrial biomass waste with natural mineral additives," *Industrial Crops and Products*, vol. 216, no. 118798, 2024.

[28] Zheng, Y., Wang, J., Wang, D., and Zheng, Z., "Advanced catalytic upgrading of biomass pyrolysis vapor to bio-aromatics hydrocarbon: A review," *Applications in Energy and Combustion Science*, vol. 10, no. 100061, 2022.

[29] Schulz, Hans F., and Jens H. Weitkamp., "Zeolite catalysts. Hydrocracking and hydroisomerization of n-dodecane," *Industrial & Engineering Chemistry Product Research and Development*, vol. 11, no. 1, pp. 46-53, 1972.

[30] Aboul-Eneın, A. A., Awadallah, A. E., El-Desoukı, D. S., and Aboul-Gheıt, N. A., "Catalytic pyrolysis of sugarcane bagasse by zeolite catalyst for the production of multi-walled carbon nanotubes." *Journal of Fuel Chemistry and Technology*, vol. 49, no. 10, pp. 1421-1434, 2021.